Solution Conformations of the Substrates and Inhibitor of Hepatitis C Virus NS3 Protease

Jung-Hoon Lee, Keunsu Bang,* Jin-Won Jung, In-Ae Ahn,† Seonggu Ro,* and Weontae Lee*

Department of Biochemistry, College of Science, Yonsei University, Seoul 120-740, Korea
†Biotech Research Institute, LG Chem. Research Park, P.O. Box 61, Yu-Sung, Science Town, Taejon 305-380, Korea
Received January 19, 1999

Hepatitis C virus (HCV) has been known to be an enveloped virus with a positive strand RNA genome and the major agent of the vast majority of transfusion associated cases of hepatitis. For viral replication, HCV structural proteins are first processed by host cell signal peptidases and NS2/NS3 site of the nonstructural protein is cleaved by a zinc-dependent protease NS2 with N-terminal NS3. The four remaining junctions are cleaved by a separate NS3 protease. The solution conformations of NS4B/5A, NS5A/5B substrates and NS5A/5B inhibitor have been determined by two-dimensional nuclear magnetic resonance (NMR) spectroscopy. NMR data suggested that the both NS5A/5B substrate and inhibitor appeared to have a folded turn-like conformation not only between P1 and P6 position but also C-terminal region, whereas the NS4B/5A substrate exhibited mostly extended conformation. In addition, we have found that the conformation of the NS5A/5B inhibitor slightly differs from that of NS5A/5B substrate peptide, suggesting different binding mode for NS3 protease. These findings will be of importance for designing efficient inhibitor to suppress HCV processing.

Introduction

Hepatitis C virus (HCV) which is an enveloped virus with a positive strand RNA genome of about 9.4 kb in length is the major agent of the vast majority of transfusion associated cases of hepatitis. HCV has also been considered as the cause in many sporadic cases of non-A and non-B hepatitis.[1-4] For viral replication, nine distinctive polypeptide products are generated through HCV processing.[5,6] It has also been reported that NS3/NS4A cleavage occurs in *cis*, whereas the others do in *trans*. In addition, the cleavage product NS4A has been found to be an integral part of NS3 as well as to increase proteolytic activity of NS3 during cleavage event.[7] Very interestingly, it has been proven that NS4A forms a complex with NS3 and accelerates the rate of cleavage at the NS5A/5B junction.[6] Recent studies also reported that the conserved residues at cleavage sites for all HCV strains played an important role to determine NS3 substrate specificity, which is an acidic residue at the P6 position, a Cys/Thr at the P1 and a Ser/Ala residue at the P1' site, respectively (Figure 1).

Very recently, X-ray crystallographic structures of not only NS3 protease domain[8] but also its complex with a synthetic 19-residue cofactor peptide[9] have been reported. The crystal structures increased our understanding for the substrate specificity of the NS3 protease as well as the structural role of cofactor NS4A. However, no solution conformational studies for neither NS3 substrate nor inhibitor based on NMR experiments have been reported yet. Since the cleavage process of the NS4B/5A substrate requires the cofactor NS4A, whereas both NS4A/4B and NS5A/5B are cleaved successfully only by NS3 protease. Therefore, it is of interest to study solution conformations of these two different substrates together with that of inhibitor. For this purpose, we have synthesized three oligopeptides, which corre-spond to sequences of NS4B/5A, NS5A/5B substrate as well as NS5A/5B inhibitor. These peptides could be used as structural references for probing the proteolytic mechanism of substrates during NS3 protease processing. In addition, the NS5A/5B inhibitor may be directly used as a good starting material for the structure-based-drug-design in developing effective anti-HCV therapy agent. Here, we report the solution conformations of NS4B/5A and NS5A/5B substrates as well as an inhibitor peptide based on two-dimensional NMR spectroscopy. In addition, we suggest the possible binding mode of the inhibitor to NS3 protein by molecular modeling calculations.

Experimental Section

Peptide Synthesis. Two 20-residue peptides which are HCV-JT type NS4B/5A substrate (Ile-Asn-Glu-Asp-Cys-

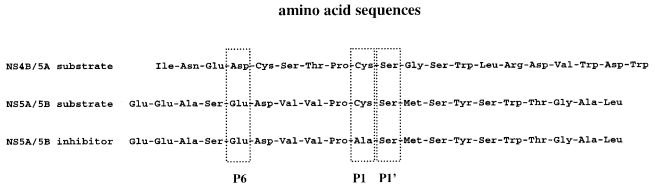

Figure 1. Amino acid sequences of the NS4B/5A, NS5A/5B substrate and NS5A/5B inhibitor indicating cleavage sites.

*To whom correspondence should be addressed: Department of Biochemistry, College of Science, Yonsei University, Shinchon-Dong, Seodaemoon-Gu, Seoul 120-740, Korea. Tel: +82-2-361-2706, Fax: +82-2-362-9897, e-mail: wlee@netstis.yonsei.ac.kr.

Ser-Thr-Pro-Cys-Ser-Gly-Ser-Trp-Leu-Arg-Asp-Val-Trp-Asp-Trp) corresponding to residues 1964-1983 of the HCV polyprotein and HCV-BK type NS5A/5B substrate (Glu-Glu-Ala-Ser-Glu-Asp-Val-Val-Pro-Cys-Ser-Met-Ser-Tyr-Ser-Trp-Thr-Gly-Ala- Leu) corresponding to 2410-2429 residues have been synthesized on the ABI-431A peptide synthesizer. In addition, an inhibitor peptide by replacing a cystein residue at P1 site to alanine from NS5A/5B substrate sequence has been synthesized. The Fmoc-protected amino acids were coupled to the Wang resin using a ABI program to suit a Fmoc coupling procedure. Purification of the synthetic peptides was achieved by equilibrating the column with 0.1% TFA in water and developing with a linear gradient of acetonitrile. All of the purified peptides were finally characterized by combined use of high pressure liquid chromatography (HPLC) and mass spectrometry (MS). The purified peptides were prepared for both NMR experiments and NS3 protease assay.

Biological Tests. The biological activities of the three synthetic peptides were examined using the truncated NS3 (tNS3) protein as previously described.[10] Both cleaved and uncleaved products of both NS4B/5A and NS5A/5B substrates were analyzed by HPLC profile. The inhibitor peptide demonstrated an inhibition activity for NS3 processing. The cofactor NS4A influence during the substrate cleavage processing has also been tested from activity differences of tNS3 protease by addition of the cofactor NS4A peptide to the substrate and tNS3 enzyme mixture.

NMR Spectroscopy. The peptide samples for NMR measurements were dissolved in either H_2O or D_2O solutions in 20 mM sodium phosphate, 2 mM DTT, 50 mM NaCl and pH value of 7.0. The final peptide concentration was 2-4 mM in 0.5 mL buffer solution. All NMR experiments were performed on a Bruker DMX-600 spectrometer in quadrature detection mode equipped with a triple resonance probe having an actively shielded pulsed-field gradient (PFG) coil. Most of experiments were performed at either 5 °C or 10 °C and the temperature were calibrated using a methanol standard.[11] Pulsed-field gradient techniques were used for all H_2O experiments, resulting in a good suppression of the solvent signal. Mixing times of 200, 400, 500 and 800 ms were used in collecting NOE spectra.[12] Total correlation spectroscopy (TOCSY)[13] data were also recorded in H_2O solution with a mixing time of 78 ms using MLEV17 spin lock pulses. Double quantum-filtered (DQF) COSY[14] spectra were collected in H_2O solution to get vicinal coupling constant information. All data were recorded in the phase sensitive mode using the time proportional phase incrementation (TPPI) method[15] with 2048 data points in the t_2 domain and 512 or 256 in the t_1 domain. Additional NOESY experiment was performed to identify slowly ex-changing amide hydrogen resonances on a freshly prepared D_2O solution after lyophilization of an H_2O sample.

All NMR data were processed using nmrPipe/nmrDraw (Biosym/Molecular Simulations, Inc.) or XWIN-NMR (Bruker Instruments) software on a SGI Indigo^2 workstation. Prior to Fourier transformation in the t_1 dimension, the first row was half-weighted to suppress t_1 ridges.[16] The DQF-COSY data were processed to 8192×1024 data matrices to get a maximum digital resolution for coupling constant measurements. The proton chemical shifts were referenced with internal sodium 4,4-dimethyl-4-silapentane 1-sulfonate (DSS).

Structure Generations. Structural calculations were performed for the inhibitor peptide using a hybrid distance geometry and dynamical simulated annealing protocol with the X-PLOR 3.1 program (Biosym/Molecular Simulations, Inc) on the SGI Indigo^2 workstation. The modeling protocol was based on the methods implemented previously by Clore and Gronenborn[17,18] with a small modification by Lee *et al.*.[19] The target function for molecular dynamics and energy minimization consisted of covalent structure, van der Waals repulsion, NOE and torsion angle constraints. The torsion angle and NOE constraints were represented by square-well potentials. Based on cross peak intensities in the NOESY spectra with mixing times of 200-800 ms, the distance constraints were classified as strong (1.8-2.7 Å), medium (1.8-3.3 Å) and weak (1.8-5.0 Å). Pseudo atom corrections were used for methylene protons, methyl groups and the ring protons of tyrosine residue. For inhibitor structure, seventy-five inter-residue distance constraints were mainly selected and used for simulated annealing calculations. Seventeen dihedral angle constraints were also deduced on the basis of the $^3J_{HN\alpha}$ coupling constants from phase-sensitive COSY spectra and used for simulated annealing calculations. A complex structure of the protease and inhibitor peptide was generated using the Docking module (InsightII) from the X-ray crystallographic data of NS3 protein (PDB entry: 1JXP) and the energy minimized average structure of the inhibitor peptide ($\langle\overline{SA}\rangle_{kl}$).

Results and Discussions

NS4B/5A Substrate. Spin system assignments were easily made from correlated cross peaks on TOCSY spectra. Single threonine, leucine and two valine residues were easily identified by their characteristic connectivities on TOCSY spectrum. Unique glycine was assigned by its distinctive fingerprint pattern in the DQF-COSY spectra. These residues were served as a starting point of sequential assignment procedure. Sequence-specific resonance assignments[20] were completed by following $d_{\alpha N}$(i,i+1) connectivities starting from NH-C$^\alpha$H cross peaks of known amino acids. The sidechain proton resonances for all residues were identified from TOCSY connectivities (Figure 2) and listed in Table 1. All of the expected $d_{\alpha N}$(i,i+1) NOEs were observed and the strong intensities of $d_{\alpha N}$(i,i+1) NOEs indicated that the NS4B/5A substrate contains a dominant population of extended conformation in aqueous solution. Pro8 has been assigned to be a *trans*-conformer based on a characteristic NOE between C$^\alpha$H of Thr7 and C$^\delta$H of Pro8. The observed inter-residue NOE connectivities for NS4B/5A substrate are summarized in Figure 3.

NS5A/5B Substrate. Spin system and sequential assignments of NS5A/5B substrate were easily completed by the

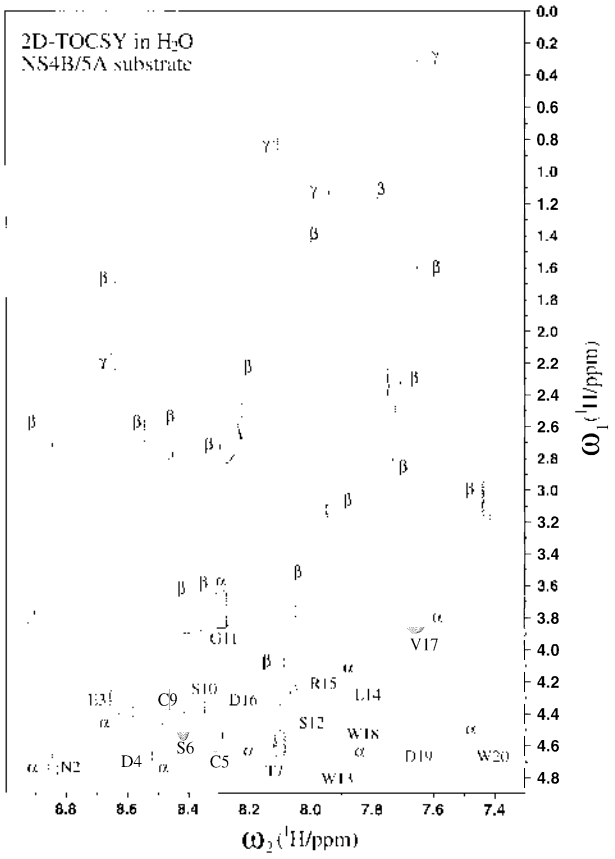

Figure 2. 600 MHz 2D-TOCSY spectrum of NS4B/5A substrate peptide in 90% H_2O/10% D_2O at pH 7.0, 10 °C, showing relayed connectivities. Spin lock time of 78 ms was used.

Figure 3. Summary of the sequential and medium range NOE connectivities identified in NS4B/5A substrate peptide. Intensities of the observed NOEs were classified by the thickness of the lines.

method described in the previous section. All proton resonances of NS5A/5B substrate were summarized in Table 1. The strong and medium intensities of the sequential $d_{\alpha N}$ (i,i+1) NOEs from all residues were observed indicating a significant population of the extended conformation in solution. However, two NH-NH NOEs which are a strong evidence of the folded structure were observed between Val7 and Val8, and between Thr17 and Gly18. In addition, a number of $d_{\beta N}$(i,i+1) NOEs were detected spanning residues from Ala3 to Thr17. The summary of the observed sequential and medium range NOE connectivities for NS5A/5B substrate is shown in Figure 4.

NS5A/5B Inhibitor. The inhibitor peptide was prepared by changing a cystein residue at P1 position to alanine in the NS5A/5B substrate. Since a residue at P1 position of substrate has been known to be crucial for NS3 processing, no

Table 1. Proton NMR chemical shifts for NS4B/5A and NS5A/5B substrates and NS5A/5B inhibitor[a]

peptides	residues	NH	$C^{\alpha}H$	$C^{\beta}H$	others
NS4B/5A substrate	Ile1		3.66	1.75	$C^{\gamma}H_2$ (1.01, 1.23) $C^{\delta}H_3$ (0.85, 1.23)
	Asn2	8.69	4.52	2.59	
	Glu3	8.51	4.14	1.73	$C^{\gamma}H_2$ (2.22)
	Asp4	8.41	4.48	2.64	
	Cys5	8.18	4.34	2.73	
	Ser6	8.32	4.29	3.68	
	Thr7	8.03	4.39	3.93	$C^{\gamma}H_3$ (1.01)
	Pro8		4.15	1.71, 2.48	$C^{\gamma}H_2$ (2.03) $C^{\delta}H_2$ (3.53)
	Cys9	8.36	4.28	2.71	
	Ser10	8.26	4.19	3.68	
	Gly11	8.20	3.64		
	Ser12	7.98	4.15	3.58	
	Trp13	7.87	4.46	3.07	2H (7.01) NH (9.99)
	Leu14	7.78	4.00	1.25	$C^{\gamma}H$ (1.08) $C^{\delta}H_3$ (0.61)
	Arg15	7.89	3.91	1.51	$C^{\gamma}H_2$ (1.28) $C^{\delta}H_2$ (2.85)
	Asp16	8.14	4.29	2.46	
	Val17	7.63	3.67	1.71	$C^{\gamma}H_3$ (0.49)
	Trp18	7.72	4.35	2.82	2H (6.89) NH (9.79)
	Asp19	7.69	4.47	2.38	
	Trp20	7.42	4.33	3.02	2H (6.73) NH (9.69)
NS5A/5B substrate	Glu1		4.02	2.15	$C^{\gamma}H_2$ (3.06)
	Glu2	8.34	4.38	1.94, 2.12	$C^{\gamma}H_2$ (2.96)
	Ala3	8.62	4.41	1.43	
	Ser4	8.37	4.65	3.91	
	Glu5	8.53	4.36	1.95	$C^{\gamma}H_2$ (2.29)
	Asp6	8.39	4.48	2.59, 2.74	
	Val7	8.05	4.14	2.07	$C^{\gamma}H_3$ (0.94)
	Val8	8.28	4.45	2.09	$C^{\gamma}H_3$ (0.99)
	Pro9		4.56	2.09, 2.34	$C^{\gamma}H_2$ (1.95, 2.05) $C^{\delta}H_2$ (3.70, 3.89)
	Cys10	8.51	4.45	2.98	
	Ser11	8.40	4.64	3.91	
	Met12	8.32	4.52	2.02, 2.10	$C^{\gamma}H_2$ (3.30)
	Ser13	8.18	4.86	3.81	
	Tyr14	8.13	4.88	2.93	2,6H (7.08) 3,5H (6.83)
	Ser15	8.13	4.85	3.81	
	Trp16	8.11	4.91	3.34	2H(7.32) 4H(7.67) 5H(7.18) 6H (7.23) 7H (7.47) NH (10.19)
	Thr17	7.94	4.25		$C^{\gamma}H_3$ (1.05)
	Gly18	7.43	3.76		
	Ala19	7.95	4.35	1.36	
	Leu20	7.86	4.23	1.61	$C^{\gamma}H$ (1.61) $C^{\delta}H_3$ (0.92)
NS5A/5B inhibitor	Glu1		4.24	1.84	$C^{\gamma}H_2$ (2.33)
	Glu2	8.31	4.27	1.85	$C^{\gamma}H_2$ (2.31)
	Ala3	8.53	4.17	1.25	
	Ser4	8.29	4.25	3.64, 3.77	
	Glu5	8.75	4.27	1.84	$C^{\gamma}H_2$ (2.32)
	Asp6	8.28	4.54	2.57, 2.68	
	Val7	7.99	3.97	1.89	$C^{\gamma}H_3$ (0.76)
	Val8	8.24	4.25	1.91	$C^{\gamma}H_3$ (0.79)
	Pro9		4.22	1.89, 2.18	$C^{\gamma}H_2$ (1.77, 1.83) $C^{\delta}H_2$ (3.60, 3.88)
	Ala10	8.38	4.11	1.28	
	Ser11	8.18	4.20	3.65, 3.76	
	Met12	8.21	4.39	1.77, 1.87	$C^{\gamma}H_2$ (2.40)
	Ser13	8.03	4.17	3.58	
	Tyr14	8.09	4.36	2.66	2,6H (6.84) 3,5H (6.61)
	Ser15	7.99	4.22	3.57	
	Trp16	7.89	4.51	3.16, 3.21	2H(7.11) 4H(7.51) 5H(7.01) 6H (7.07) 7H (7.25) NH (10.00)
	Thr17	7.85	4.19	3.92, 4.05	$C^{\gamma}H_3$ (1.12)
	Gly18	8.09	3.68, 3.80		
	Ala19	8.23	4.26	1.27	
	Leu20	7.97	4.10	1.45	$C^{\gamma}H$ (1.45) $C^{\delta}H_3$ (0.76)

[a]Chemical shifts are expressed in ppm from internal DSS. The samples were maintained at 10 °C.

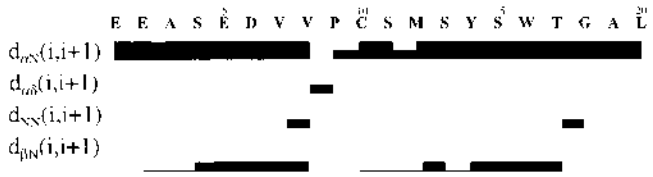

Figure 4. Summary of the sequential and medium range NOE connectivities observed in NS5A/5B substrate peptide. NOE intensities were classified by the thickness of the lines.

cleavage product from the inhibitor was observed during cleavage test as we expected. Instead, the peptide showed an inhibition activity of $K_i \sim 80\ \mu M$ for NS3 protease. A continuous stretch of $d_{\alpha N}(i,i-1)$ sequential NOEs were used for assignment procedure (Figure 5A). A number of $d_{NN}(i,i+1)$ NOEs were observed spanning residues of Asp6 to Ala19 (Figure 5B). Two $d_{NN}(i,i-1)$ NOEs, which are between Asp6 and Val7 and between Val7 and Val8, are detected consistent with a turn structure in which Asp6, Val7 and Val8 residues are involved. A $d_{\alpha N}(i,i+3)$ NOE which is indicative of β-turn was also observed between Glu5 and Val8. This result was also supported by a $d_{NN}(i,i+3)$ NOE together with $^3J_{HN\alpha}$ coupling constant data (Figure 6). In addition, a number of NOEs were observed in the C-terminal area of NS5A/5B

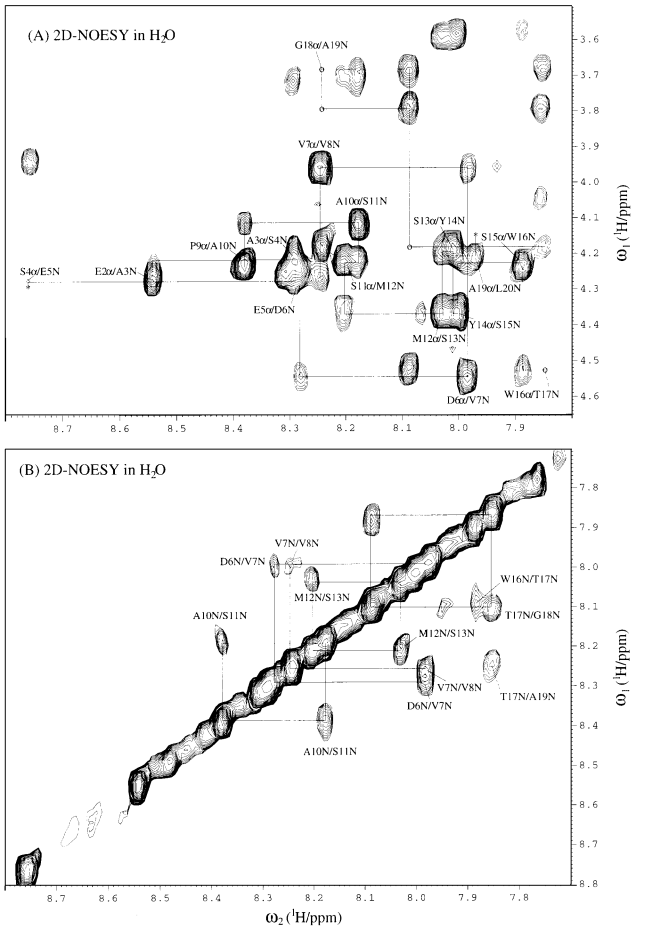

Figure 5. 2D-NOESY spectra of NS5A/5B inhibitor peptide in (A) fingerprint and (B) $d_{NN}(i,i+1)$ contact regions were displayed. The NOE mixing time of 600 ms was used.

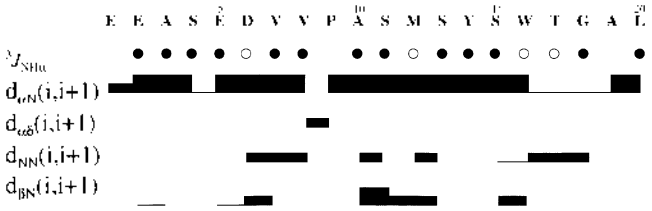

Figure 6. Summary of the sequential and medium range NOE connectivities and backbone NH-C$^\alpha$N vicinal coupling constants (● for $^3J_{HN\alpha} > 8$ Hz; ○ for $^3J_{HN\alpha} < 6$ Hz) identified in NS5A/5B inhibitor.

inhibitor. A medium $d_{NN}(i,i-1)$ NOEs between Trp16 and Thr17 and between Thr17 and Gly18 as well as a stretch of weak $d_{\alpha N}(i,i+1)$ NOEs spanning residues from Trp16 to Gly18 were observed supporting a turn conformation comprising residues Trp16, Thr17 and Gly18. As a result, it is expected that the NS5A/5B inhibitor contains a high population of the turn-forming structure spanning regions of Asp6 to Gly18. The observed sequential NOE connectivities and dihedral angle constraints for NS5A/5B inhibitor are summarized in Figure 6 and the chemical shift list is shown in Table 1. The solution structures of the NS5A/5B inhibitor were generated by the experimental constraints deduced from NMR data. Among twenty starting structures, twelve structures showed no constraint violations greater than 0.5Å for distances and 5° for torsion angles and were subjected for conformational analysis. The average structure was calculated from 12 final structure coordinates and followed restrained energy minimization procedure, generating a restrained energy minimized (REM) average structure of inhibitor peptide ($<\overline{SA}>_{kr}$) (Figure 7A). This average REM structure showed 0.95 Å RMS deviation for all backbone atoms and 1.24 Å for heavy atoms with respect to 12 $<SA>_k$ structures. Energies and structural statistics for 12 $<SA>_k$ and $<\overline{SA}>_{kr}$ structures are listed in Table 2. A complex structure of the protease-inhibitor was generated using the Docking module of InsightII program (Biosym/Molecular Simulation Inc.) from the NMR structure of inhibitor based on X-ray coordinates of NS3 (Figure 7B).

The structure of the free inhibitor peptide exhibits a kink between the P1 and P6 residue and a twisted strand in the C-terminal (Figure 7A). However, the inhibitor demonstrates a structural transition when it complexed with NS3 protein. Especially, it is noticeable that the cleavage site of the inhibitor was shifted toward the catalytic triad (His57, Asp81 and Ser139) of the protease resulting a narrow kink about P1 site (Figure 7B). It is also of interest to see that the conformation in the C-terminal region became more extended form than that of the free inhibitor alone. HCV NS3 protein has been known to hydrolyze four different cleavage sites during the maturation step. Among these cleavage sites, NS3/4A is cleaved by *cis*-cleavage through intramolecular hydrolysis. The other three sites are mediated by *trans*-cleavage which involves intermolecular hydrolysis reaction. From the sequence alignments of known cleavage sites, the substrate specificity of HCV NS3 protease have been identified. It has

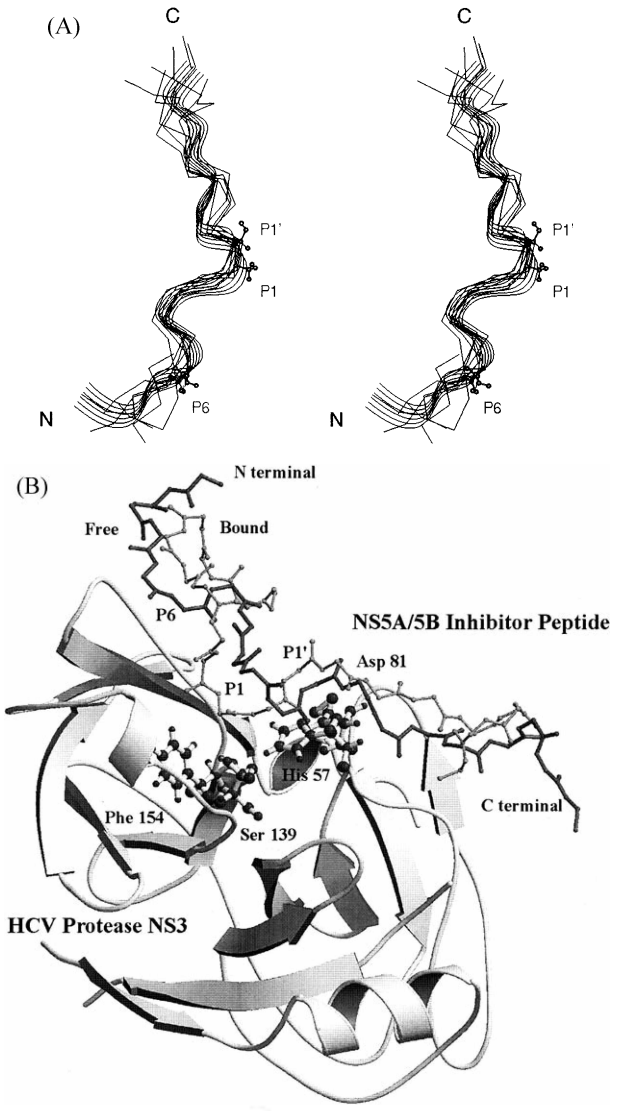

Figure 7. Model of both free and NS3 bound inhibitor peptides. (A). Superposition of the final 7 $\langle SA \rangle_k$ structures of the NS5A/5B inhibitor (in line drawing) over the energy minimized average structure (in ribbon plot) displayed in stereoview. A ball and stick model was used for displaying the side chains of P1, P1' and P6 residues. (B). Modeling structure of the NS5A/5B inhibitor complexed with NS3 protease. The backbone C^{α} trace of protease is displayed in ribbon and the inhibitor in line drawing. A P1 pocket (Phe154) and a catalytic triad residues are represented in ball and stick model. This image was generated with MOLSCRIPT[21] and rendered with Raster3D[22].

been shown that there has to be an acidic amino acid at P6, a cysteine or threonine residue at P1 and a serine or alanine residue at P1' position for efficient cleavage process, respectively (Figure 1). The mutant studies of the substrates have also demonstrated that P1 position of the substrate was crucial for all the NS3 protease processing, whereas P1' residue appeared to be less important for cleavage. In addition, it has been suggested that the acidic amino acid requirement at P6 position is not critical for substrate recognition and cleavage. It has also been reported that the cleavage process of the NS4B/5A substrate required the cofactor NS4A, whereas

Table 2. Structural statistics for the final simulated annealing structures of NS5A/5B inhibitor

	$\langle SA \rangle_k$	$\langle \overline{SA} \rangle_{kr}$
(A) RMS deviations from experimental distance restraints (Å)		
all (116)	0.0861	0.0652
sequential ($\|i-j\| = 1$) (37)	0.0972	0.0497
short range ($1 < \|i-j\| \leq 5$) (35)	0.0465	0.0313
intraresidue (44)	0.0422	0.0333
(B) RMS deviations from experimental dihedral restraints (deg)		
dihedral restraints (17)	0.2081	0.1227
(C) Energies (kcal mol^{-1})		
E_{total}	87.6	79.0
E_{NOE} (all)	45.8	34.9
E_{tor}	34.2	41.5
E_{repel}	1.4	0.9
(D) Deviations from idealized covalent geometry		
bonds (Å)	0.0075	0.0059
angles (deg)	0.7011	0.6529
impropers (deg)	0.6785	0.5564

both NS4A/4B and NS5A/5B were cleaved successfully only by NS3 protease. Thereby, our NMR data provides an explanation about this difference. Since the NOE pattern of NS4B/5A substrate which is an amide-amide NOE between Val7 and Val8, is totally different from that of NS5A/5B (Figure 6), the NS5A/5B substrate appears to have a turn-like conformation between P1 and P6 position. In contrast, the NOEs of the NS4B/5A substrate clearly supports the extended conformation (Figure 4). Very interestingly, an NH-NH NOE between Val7 and Val8 was observed in both substrate and inhibitor peptides of the NS5A/5B junction. In addition, the overall NOE pattern of both peptides is very similar each other. This indicates the existence of the folded turn type conformations in both NS5A/5B substrate and inhibitor. However, we have found that the solution conformation of NS5A/5B inhibitor in the C-terminal region is slightly different from that of NS5A/5B substrate by NOE comparison (Figure 4 and 6). Therefore, we could assume that the inhibitor peptide might have different binding modes from that of substrate for NS3 protease. The structural information of these peptides presented here will be very useful for designing efficient inhibitor to suppress HCV processing.

Acknowledgments. This work was supported by the research grant from Yonsei University (1997). The authors give thanks to Dr. Eunice E. Kim for invaluable discussions and to TMSI Korea for the providing of the molecular modeling programs (InsightII and X-PLOR 3.1), Molecular Simulations, Inc.

References

1. Purcell, R. H. *FEMS Microbiol. Rev.* **1994**, *14*, 181-192.
2. Kato, N.; Hijikata, M.; Ootsuyama, Y.; Nakagawa, M.; Ohkoshi, S.; Sugimura, T.; Shimotohno, K. *Proc. Natl. Acad. Sci. USA* **1990**, *24*, 9528.

3. Choo, Q. L.; Richman, K. H.; Han, J. H.; Berger, K.; Lee, C.; Dong, C.; Gallegos, C.; Colt, D.; Medina-Selby, A.; Barr, P. J. *Proc. Natl. Acad. Sci. USA* **1991**, *88*, 2451-2455.
4. Takamizawa, A.; Mori, C.; Fuke, I.; Manabe, S.; Murakami, S.; Fujita, J.; Onishi, E.; Andon, T.; Yoshida, I.; Okayama, H. *J. Virol.* **1991**, *65*, 1105-1113.
5. Grakoui, A.; McCourt, D. W.; Wychowski, C.; Feinstone, S. M.; Rice, C. M. *J. Virol.* **1993**, *67*, 4665-4675.
6. Hijikata, M.; Mizushima, H.; Akagi, T.; Mori, S.; Kakiuchi, N.; Kato, N.; Tanaka, T.; Kimura, K.; Shimotohno, K. *J. Virol.* **1993**, *67*, 4665-4675.
7. Simizu, Y.; Yamaji, K.; Massiho, Y.; Yokota, T.; Inoue, H.; Sudo, K.; Satoh, S.; Shimotohno, K. *J. Virol.* **1996**, *70*, 127-132.
8. Kim, J. L.; Morgenstern, K. A.; Lin, C.; Fox, T.; Dwyer, M. D.; Landro, J. A.; Chambers, S. P.; Markland, W.; Lepre, C. A.; OMalley, E. T.; Harbeson, S. L.; Rice, C. M.; Murcko, M. A.; Carson, P. R.; Thomson, J. A. *Cell* **1996**, *87*, 343-355.
9. Love, R. A.; Parge, H. E.; Wickersham, J. A.; Habuka, N.; Moomaw, E. W.; Adachi, T.; Hostomska, *Z. Cell* **1996**, *87*, 331-342.
10. Grakoui, A.; McCourt, D. W.; Wychowski, C.; Feinstone, S. M.; Rice, C. M. *J. Virol.* **1993**, *67*, 2832-2843.
11. Van Geet, A. L. *Analyt. Chem.* **1970**, *42*, 679-680.
12. Jeener, J. Meier, B. H.; Bachmann, P.; Ernst, R. R. *J. Chem. Phys.* **1979**, *71*, 4546-4553.
13. Davis, D. G.; Bax, A. *J. Am. Chem. Soc.* **1985**, *107*, 2820- 2823.
14. Piantini, U.; Sorensen, O. W.; Ernst, R. R. *J. Am. Chem. Soc.* **1982**, *104*, 6900-6901.
15. Marion, D.; Wuthrich, K. *Biochem. Biophys. Res. Commun.* **1983**, *113*, 967-974.
16. Otting, G.; Widmer, H.; Wagner, G.; Wuthrich, K. *J. Magn. Reson.* **1986**, *66*, 187-193.
17. Driscoll, P. C.; Gronenborn, A. M.; Beress, L.; Clore, G. M. *Biochemistry* **1989**, *28*, 2188-2198.
18. Nilges, M.; Clore, G. M.; Gronenborn, A. M. *FEBS Lett.* **1988**, *229*, 317-324.
19. Lee, W.; Moore, C. H.; Watt, D. D.; Krishna, N. R. *Eur. J. Biochem.* **1994**, *218*, 98-95.
20. Wuthrich, K. *NMR of Proteins and Nucleic Acids*; Wiley: New York, 1986.
21. Kraulis, P. J. *J. Appl. Cryst.* **1991**, *24*, 946-950.
22. Merritt, E. A.; Bacon, D. J. *Methods in Enzymology* **1997**, *277*, 505-524.